
DEPARTMENT OF THE INTERIOR

U.S. GEOLOGICAL SURVEY

**PRISM 8° x 10° Northern Hemisphere
Paleoclimate Reconstruction: Digital Data**

PRISM Project Members



Open-File Report 94-281

This report is preliminary and has not been reviewed for conformity
with U.S. Geological Survey editorial standards

PRISM 8°x10° Northern Hemisphere Paleoclimate Reconstruction: Digital Data

Prism Project Members¹

Introduction

The PRISM 8°x10° data set represents several years of investigation by PRISM (Pliocene Research, Interpretation, and Synoptic Mapping) Project members. One of the goals of PRISM is to produce time-slice reconstructions of intervals of warmer than modern climate within the Pliocene Epoch. The first of these was chosen to be at 3.0 Ma (time scale of Berggren et al., 1985) and is published in *Global and Planetary Change* (Dowsett et al., in press). This document contains the actual data sets and a brief explanation of how they were constructed. For paleoenvironmental interpretations and discussion of each data set, see Dowsett et al., in press. The data sets includes sea level, land ice distribution, vegetation or land cover, sea surface temperature and sea-ice cover matrices.

General Description

This reconstruction of middle-Pliocene climate is organized as a series of datasets representing different environmental attributes. The data sets are designed for use with the GISS Model II atmospheric general circulation model (GCM) using an 8°x10° resolution (Hansen et al., 1983). The first step in documenting the Pliocene climate involves assigning an appropriate fraction of land versus ocean to each grid box (Figure 1). Following grid cell by grid cell, land versus ocean allocations, winter and summer sea ice coverage of ocean areas are assigned and then winter and summer sea surface temperatures are assigned to open ocean areas. Average land ice cover is recorded for land areas and then land areas not covered by ice are assigned proportions of six vegetation or land cover categories modified from Hansen et al. (1983). In the example shown in Figure 1, the cell centered at 58.77° North latitude and 140° West longitude (row 20, column 5) has 40% land coverage and 60% water coverage. The water area in the cell is assigned winter (February) and summer (August) sea surface temperature (SST) values of 8.6°C and 15.9°C respectively. The land area in the cell has no land ice cover nor does the water have any sea ice cover. Of the six land cover or vegetation types in Table 1, the land area of this cell is covered 20% by deciduous forest and 80% by evergreen vegetation.

Sea Level

We constructed an 8°x10° grid of estimated Pliocene sea-level by determining the +25 m elevation in the NOAA ETOPO5 5-minute bathymetry/topography digital relief data set of the world². Each elevational value in the ETOPO5 grid was converted to

¹Contributors to this report in alphabetical order: John A. Barron, Thomas M. Cronin, Harry J. Dowsett, Farley R. Fleming, Thomas R. Holtz, Jr., Scott E. Ishman, Richard Z. Poore, Robert S. Thompson, Debra A. Willard.

²NOAA National Geophysical Data Center Data Announcement 88-MGG-02.

either a value of one (the grid point was at or above +25 m elevation) or zero (the grid point was below +25 m). A $1^{\circ}\times 1^{\circ}$ "presence-absence" grid for land was constructed by determining the percentage of land within a given $1^{\circ}\times 1^{\circ}$ cell by summing the number of 1's (from the 5-minute data) and dividing by the total number of grid points (144). If the percentage value was less than 50% land, then the cell was declared to be water and assigned a zero in the $1^{\circ}\times 1^{\circ}$ grid. If the percentage of land was 50% or greater, then the cell was declared to be land and assigned a value of one in the $1^{\circ}\times 1^{\circ}$ grid. The $1^{\circ}\times 1^{\circ}$ presence-absence matrix was then processed at NASA-GISS to produce an $8^{\circ}\times 10^{\circ}$ percentage matrix (Fig. 2). The percentage of land in each cell is scaled from 0 to 1.0 (complete coverage). These estimates of coastline changes are based solely on elevation data and do not take into account isostatic rebound associated with melting of ice sheets nor elevation changes due to tectonic adjustments occurring since the Pliocene.

Sea Surface Temperature (SST)

SST data sets provide Pliocene surface temperatures for February and March (Figs. 3-4). Temperatures range from -1.56°C (sea-ice) to 30°C . We constructed February and August SST data sets by determining the deviation from modern conditions for all marine localities using quantitative and qualitative assemblage data from planktic foraminifers, diatoms, and ostracodes (Dowsett et al., in press). We then contoured and smoothed these deviations for February and August to create $8^{\circ}\times 10^{\circ}$ February and August anomaly maps. These anomalies were applied to modern SST files to create Pliocene February and August SST Files (Figs. 3-4).

Sea Ice Distribution

For Pliocene Northern Hemisphere winter we used modern summer (August 1 through August 15) sea-ice conditions (U.S. Navy Hydrographic Office, 1958); average sea-ice concentrations ≥ 0.5 were used to approximate the modern average ice open-water margin. The position of that margin in each $8^{\circ}\times 10^{\circ}$ grid cell determined the geographic coverage in the cell. Cells with complete sea-ice cover were coded as 1.0, while cells with no sea-ice cover were coded as 0.0 (Fig. 5). Our Pliocene summer reconstruction incorporates an ice-free Arctic Ocean, thus Northern Hemisphere grid cells containing ocean were coded as 0.0 indicating no coverage by sea-ice (Fig. 6).

Pliocene sea-ice limits for the Southern Hemisphere (circumantarctic) were estimated on the basis of existing Pliocene sea-surface temperature (SST) and mean annual surface air temperature estimates. We estimated winter (August) sea-ice limits to be similar to modern summer (February) conditions. Average circumantarctic sea-ice concentrations of $\geq 0.6^3$ were used to approximate the modern average ice-open water margin (Naval Oceanography Command Detachment, 1985). The position of that margin in each $8^{\circ}\times 10^{\circ}$ grid cell determined the geographic coverage in the cell. Cells with complete sea-ice cover were coded as 1.0 while cells with no sea-ice cover were coded as 0.0 (Fig. 6). As with the Northern Hemisphere, we assume the circumantarctic was ice-free during the austral summer (February) (Fig. 5).

Land Ice Distribution

³Northern and southern hemisphere sea-ice atlases use different sea ice concentration cutoffs. Thus we used the ≥ 0.5 concentration for the northern hemisphere and ≥ 0.6 concentration in the southern hemisphere to denote the sea-ice open-water margin.

The Land Ice distribution data set provides information on Pliocene land-ice coverage (Fig. 7). Grid cells completely covered by land ice are coded with 1, cells without land ice are coded with 0. As discussed in Dowsett et al., in press, we effectively removed all Northern Hemisphere land ice except for 50% of the aerial cover of Greenland. We modified the modern distribution of ice in southern hemisphere cells of the $8^{\circ}\times 10^{\circ}$ grid using the Oerlemans (1982) models as a guide to represent removal of the West Antarctic ice sheet and 25% reduction in the size of the East Antarctic ice sheet (Figure 7). This land ice reduction provides the necessary sea level rise for our sea level reconstruction.

Land Vegetation

The GISS model uses an eight-type vegetation classification to provide hydrological and albedo parameters for model simulations (Hansen et al., 1983). Desert, tundra, grassland, shrub grassland, tree grassland, deciduous forest, evergreen forest, and rainforest are expressed as a percentage of the total land cover in each cell containing land. For modern vegetation, these percentages were obtained from a $1^{\circ}\times 1^{\circ}$ grid of 22 possible vegetation types (Matthews, 1985) in which each cell is characterized by a single vegetation type. For the $8^{\circ}\times 10^{\circ}$ grid these $1^{\circ}\times 1^{\circ}$ cells are summed and divided by the total number of cells to produce matrices of percentage of total land cover for each vegetation class. We determined that it was too difficult to discern the differences among the three grassland categories (all of which have similar albedo and hydrology characteristics in the GISS parameterization) in the fossil data, and thus these three classes were summed into a single "total grassland" category.

To construct the Pliocene $8^{\circ}\times 10^{\circ}$ vegetation grid we adjusted the values in the modern grid to fit the broad geographic patterns in Pliocene vegetation apparent in the paleobotanical data described in Dowsett et al., in press. The modern value for an individual cell was adjusted by taking into account what is known about Pliocene vegetation in that cell (or if no data were available from that cell, from the nearest cell with data). The modern and Pliocene vegetation on the GISS grid are presented in Table 1.

Desert. The desert category in the modern $8^{\circ}\times 10^{\circ}$ grid has two components — polar desert and middle or low latitude desert. These vegetation associations are grouped together for the numerical climate model because they have similar albedo and hydrological characteristics. In the absence of data constraining the areal extent of deserts we reduced the areal extents around the peripheries of the modern deserts and approximately halved their modern proportions within the other modern desert cells (Figure 8, Table 1). The reductions in desert were largely made up by increasing grassland/steppe proportions with these grid cells (see discussion below).

Tundra. For the GISS $8^{\circ}\times 10^{\circ}$ Pliocene vegetation grid, we concluded that tundra was quite restricted at 3.0 Ma and it was entered as low levels of abundance in the northernmost two rows of cells (Figure 9, Table 1).

Evergreen Forest. For the Pliocene $8^{\circ}\times 10^{\circ}$ vegetation grid (Figure 10, Table 1) evergreen forest was entered at high abundance in the higher latitude of North America and Eurasia. In the western United States, Europe and southwestern and central Asia, the percentage of evergreen vegetation was increased (relative to modern) and its range extended.

Deciduous Forest. We maintained the current centers of high abundance for deciduous vegetation in the $8^{\circ}\times 10^{\circ}$ Pliocene vegetation grid (Figure 11, Table 1). These persistent 'centers of mass' for this vegetation category occur in eastern North America, northwest Europe, and southern Asia. In addition, Pliocene deciduous vegetation was increased

(relative to today) in the circum-Mediterranean region and east Africa. To reflect the occurrence of deciduous trees in Pliocene boreal and temperate conifer forests, low levels of deciduous vegetation were coded into grid cells as far north as the latitude of the North Slope of Alaska.

Grassland. Grassland as used here combines the GISS categories of grassland, shrub-grassland (steppe), and tree-grassland (savanna) (Figure 12, Table 1). For the Pliocene, modern grassland and steppe vegetation was maintained at reduced abundance in central North America and in parts of central Asia and Africa. The abundance of the grassland category was increased for the modern mid/low latitude desert regions (see discussion in Dowsett et al., in press).

Rain Forest. For the 8°x10° grid (Figure 13, Table 1), the modern distribution of rain forest was used with only minor modification for smoothness.

Data Availability

These data and this report are available through the USGS Global Change and Climate History Program Global Change Database. Use anonymous FTP to geochange.er.usgs.gov.

Bibliography

- Berggren, W.A., Kent, D.V., and Van Couvering, J.A., 1985. Neogene geochronology and chronostratigraphy In: N.J. Snelling (Editor), The Chronology of the Geological Record. London, Blackwell Scientific Publications, pp. 211-260.
- Dowsett, H.J., Thompson, R.S., Barron, J.A., Cronin, T.M., Fleming, F., Ishman, S.E., Poore, R.Z., Willard, D.A. and Holtz, T.R., Jr., in press. Paleoclimate reconstruction of a warmer Earth: PRISM Middle Pliocene Northern Hemisphere synthesis. *Global and Planetary Change* : 49pp.
- Hansen, J., Russell, G., Rind, D., Stone, P., Lacis, A., Lebedeff, S., Ruedy, R., Travis, L., 1983. Efficient three-dimensional global models for climate studies: models I and II. *Monthly Weather Review* 111(4): 609-662.
- Matthews, E., 1985. Prescription of land-surface boundary conditions in GISS GCM II: a simple method based on high-resolution vegetation data bases. NASA Report No. TM 86096 : 20 p.
- Naval Oceanography Command Detachment, 1985. Sea Ice Climate Atlas, vol. 1, Antarctica. NAVAIR 50-1C-540.
- Oerlemans, J., 1982. Response of the Antarctic ice sheet to a climatic warming: a model study. *Journal of Climatology*, 2: 1-11.
- U.S. Navy Hydrographic Office, 1958. Oceanographic Atlas of the Polar Seas, Part II: Arctic.

Appendix 1 PRISM PROJECT MEMBERS

Names and addresses are provided as points of contact for various data sets discussed above. Areas of specific knowledge for both underlying science and data manipulation associated with each data set are given using the following codes: ST for Sea Surface Temperature; SI for Sea Ice; SL for Sea Level; VG for Vegetation; LI for Land Ice; OV for general overview of all data sets.

John A. Barron [ST,SI,SL]
USGS MS 915
345 Middlefield Rd.
Menlo Park, CA 94025

jbarron@isd.mnl.wr.usgs.gov
(415)329-4971

Thomas M. Cronin [ST,SI,SL]
USGS
970 National Center
Reston, VA 22092

tcronin@geochange.er.usgs.gov
(703)648-6363

Harry J. Dowsett [ST,SL,OV]
USGS
970 National Center
Reston, VA 22092

hdowsett@geochange.er.usgs.gov
(703)648-5282

Farley R. Fleming [VG]
USGS
919 Federal Center
Denver, CO 80225

ffleming@greenwood.cr.usgs.gov
(303)236-5681

Scott E. Ishman [LI,SI]
USGS
970 National Center
Reston, VA 22092

sishman@geochange.er.usgs.gov
(703)648-5316

Richard Z. Poore [ST,SI]
USGS
955 National Center
Reston, VA 22092

rpoore@geochange.er.usgs.gov
(703)648-5270

Robert S. Thompson [VG,SL,OV]
USGS
919 Federal Center
Denver, CO 80225

thompson@greenwood.cr.usgs.gov
(303)236-0439

Debra A. Willard [VG]
USGS
970 National Center
Reston, VA 22092

dwillard@geochange.er.usgs.gov
(703)648-5320

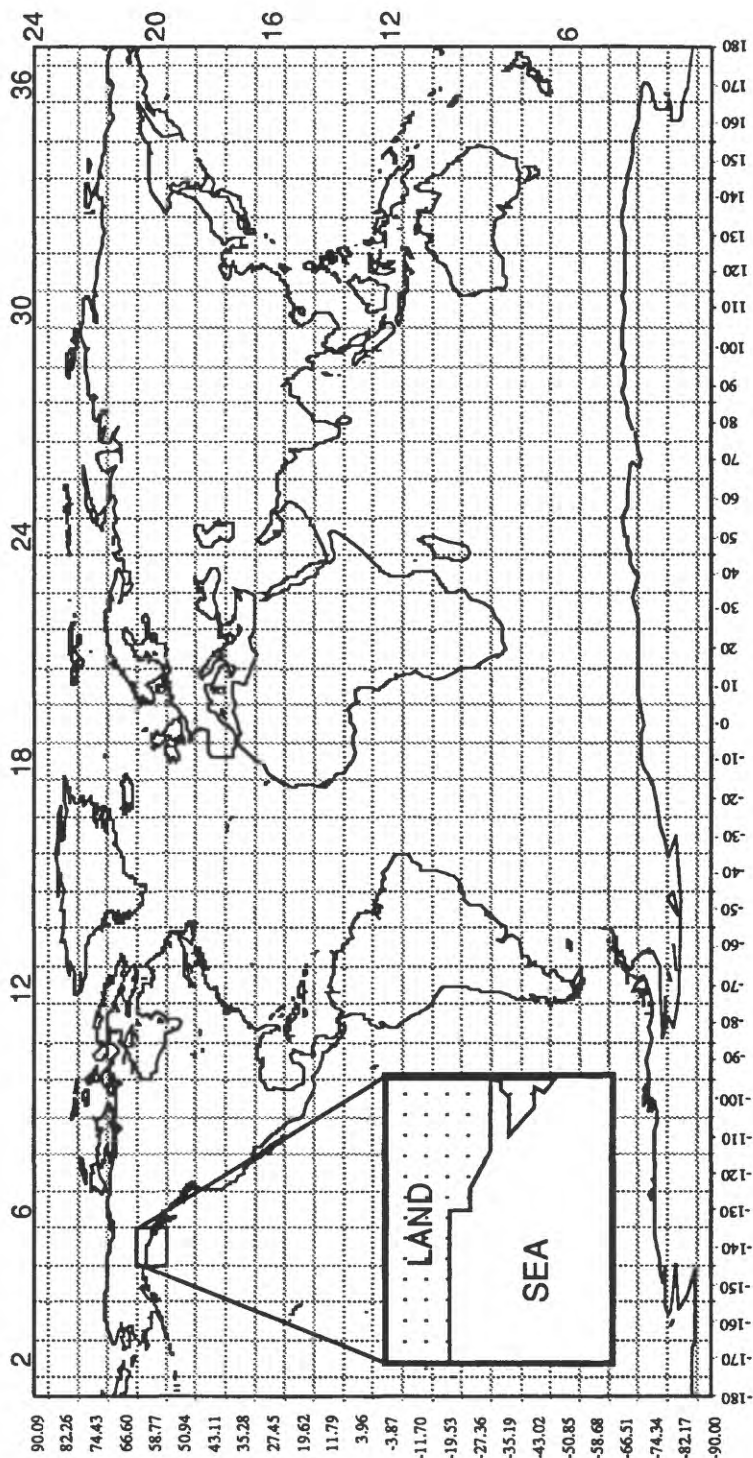


Figure 1. World map showing 8° by 10° grid system used in this reconstruction. Each cell can be designated by its latitudinal and longitudinal midpoints (left and bottom axes) or by a scheme using latitude row and longitude column numbers (right and top axes). The expanded cell is identified as either latitude 58.77, longitude -140.00, or row 20, column 5.

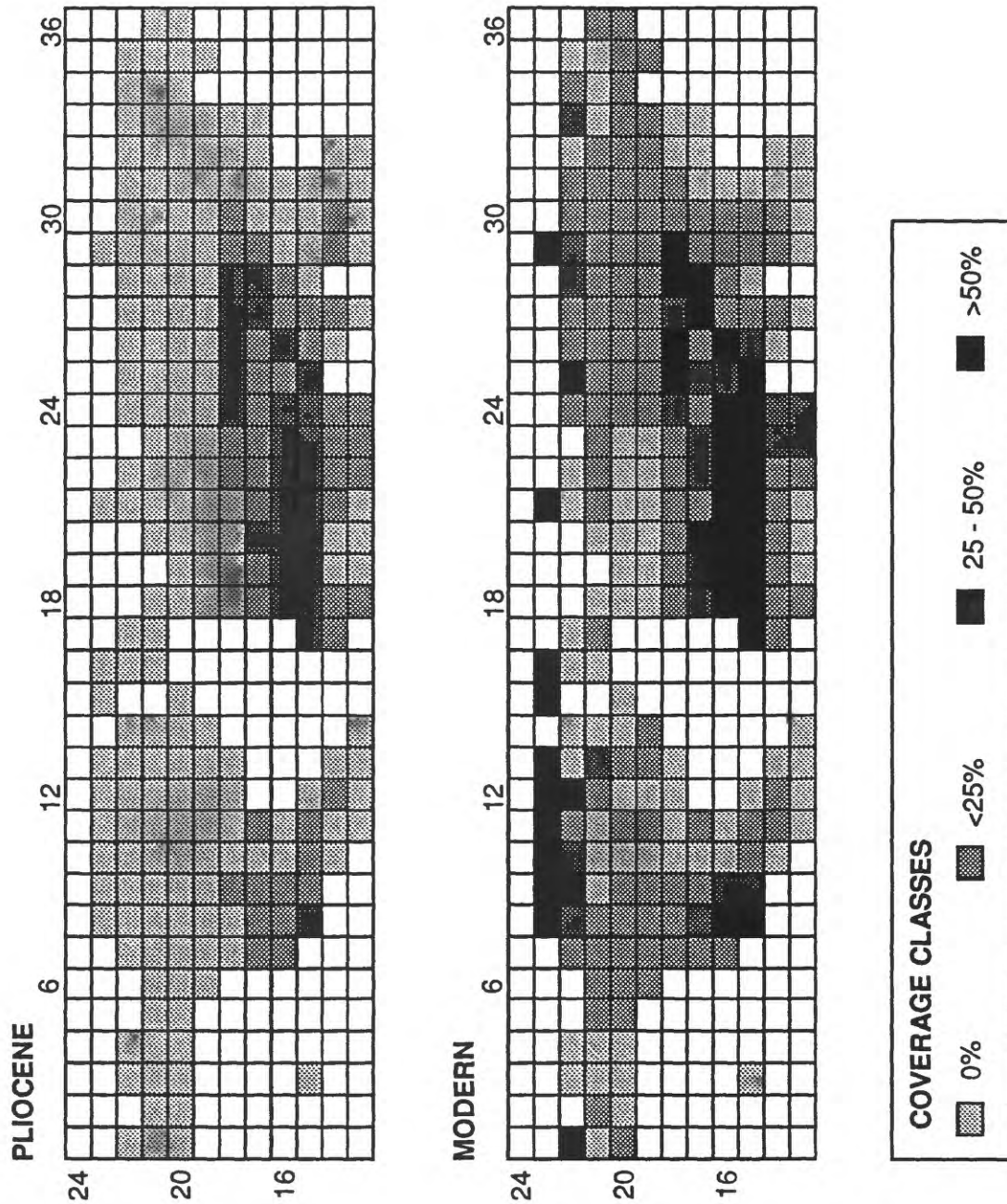


Figure 8. Desert vegetation

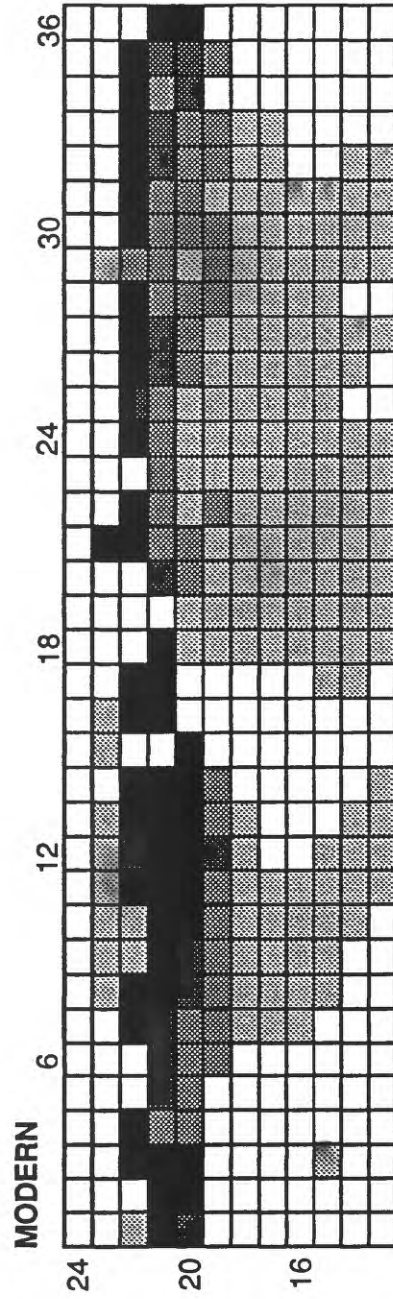
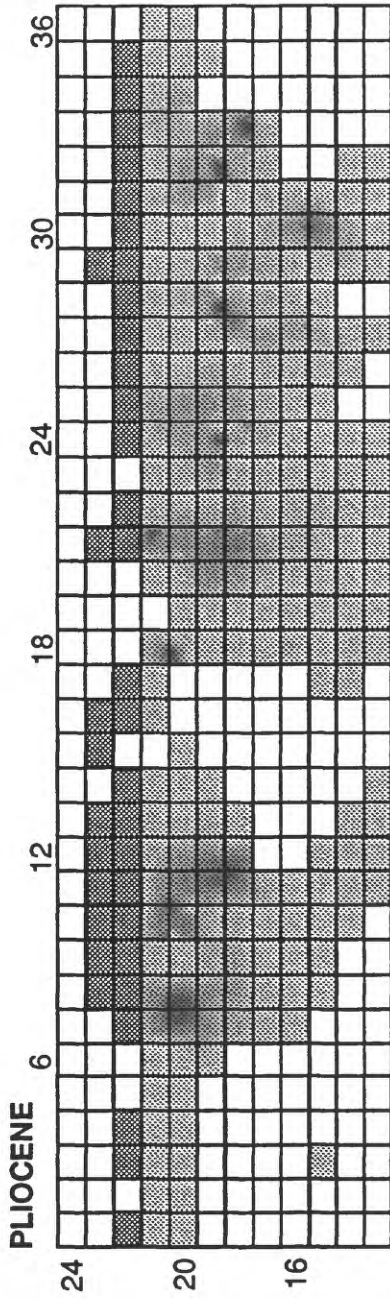


Figure 9. Tundra vegetation

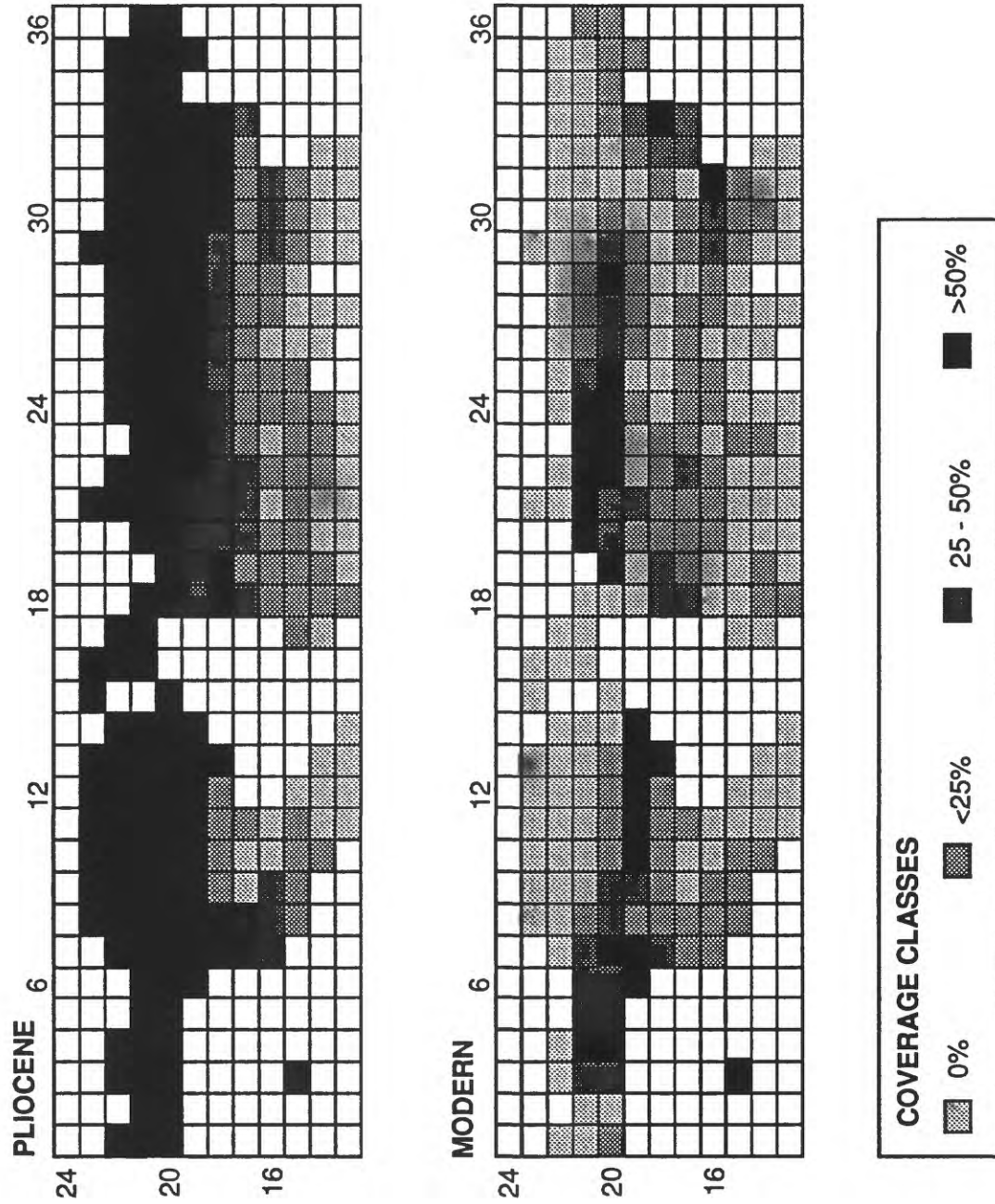


Figure 10. Evergreen forest vegetation

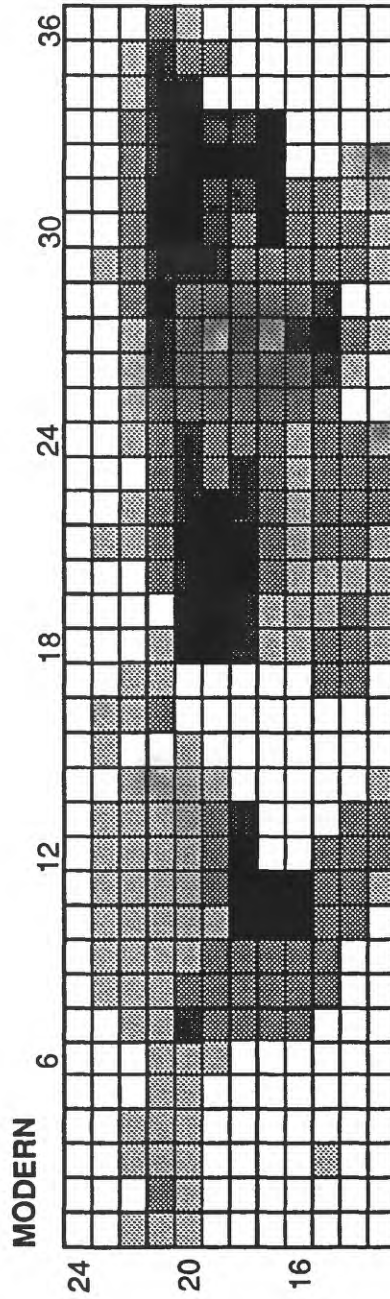
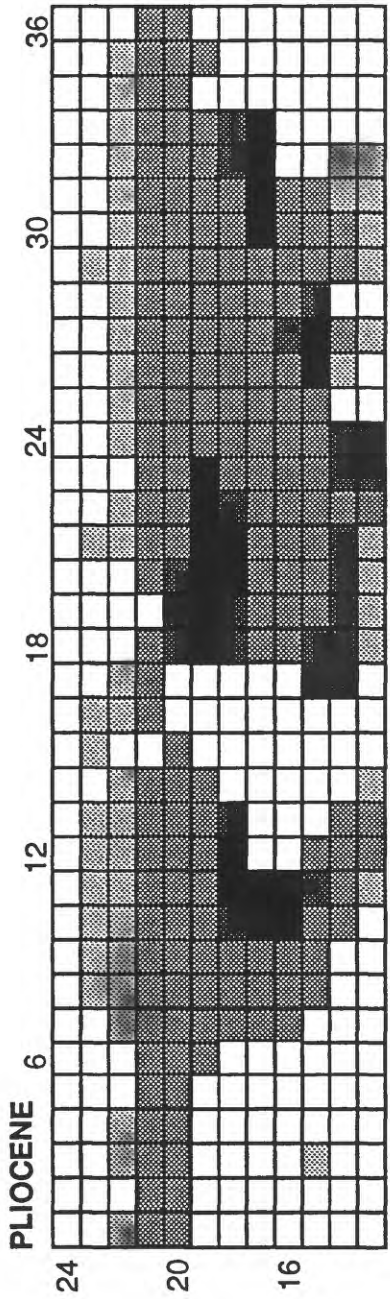


Figure 11. Deciduous forest vegetation

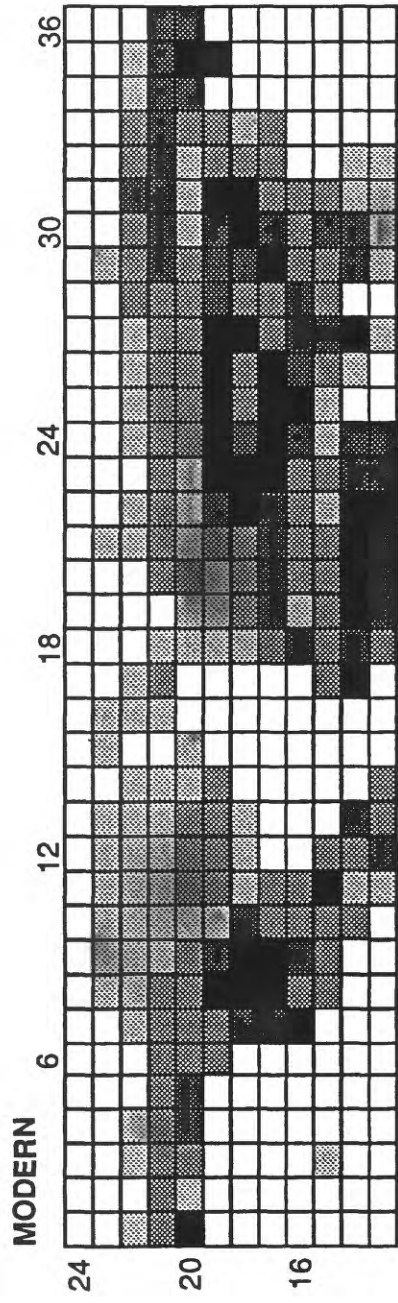
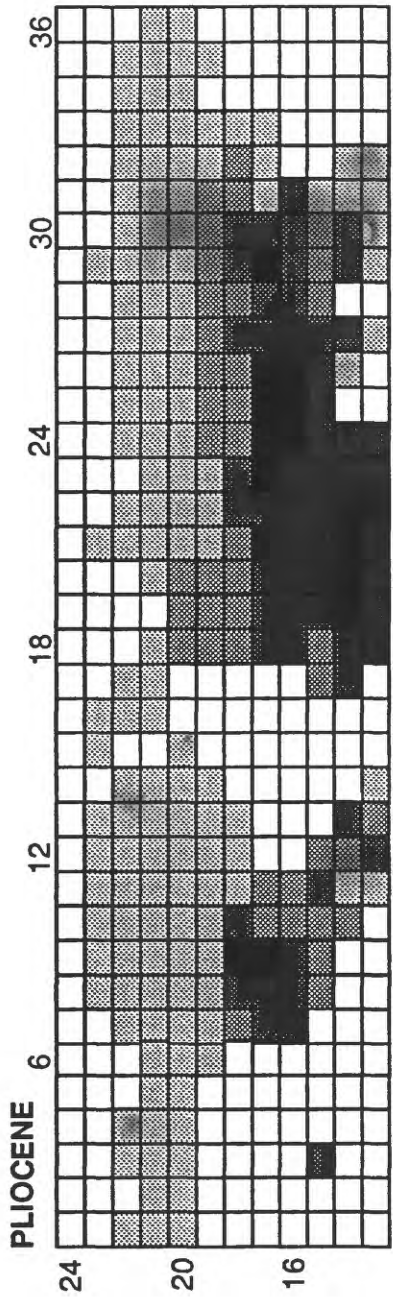


Figure 12. Grassland vegetation

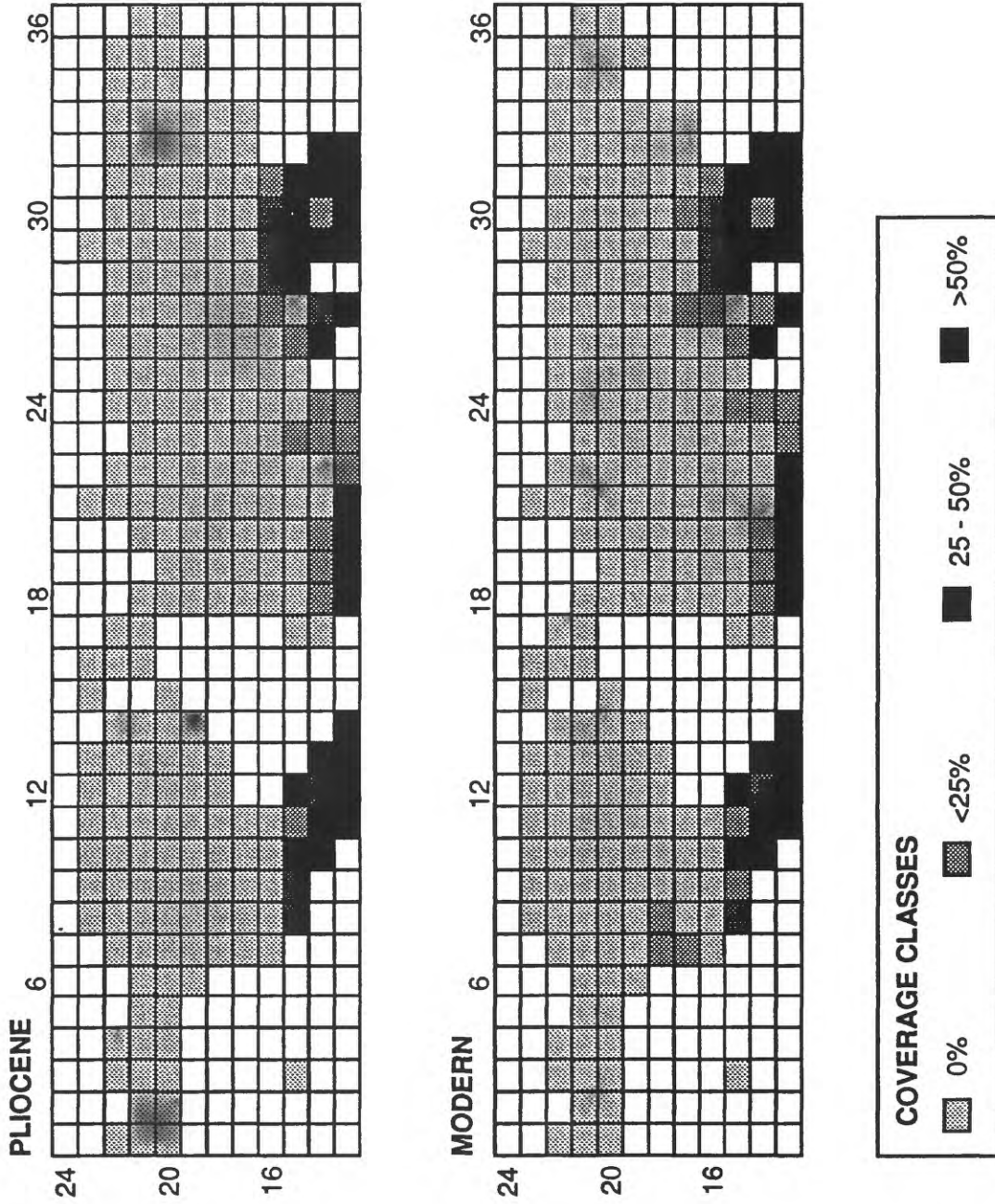


Figure 13. Rain forest vegetation

Table 1. Modern (left) and corresponding Pliocene (right) vegetation for land cells in the GISS 8°X10° grid. Each cell is identified by its latitude/longitude position in the grid (in the farthest left column the first two digits refer to the latitude row, and the last two digits refer to the longitude column in the GISS 8°X10° grid). The vegetation for each cell is expressed as percentages of ground cover for six vegetation categories (DES=desert, TUN=tundra, EVE=evergreen forest, DEC=deciduous, GRA=grassland, RAI=rainforest).

LatLon	MODERN						PLIOCENE					
	DES	TUN	EVE	DEC	GRA	RAI	DES	TUN	EVE	DEC	GRA	RAI
2308	100	0	0	0	0	0	0	25	75	0	0	0
2309	100	0	0	0	0	0	0	25	75	0	0	0
2310	100	0	0	0	0	0	0	25	75	0	0	0
2311	100	0	0	0	0	0	0	25	75	0	0	0
2312	100	0	0	0	0	0	0	25	75	0	0	0
2313	100	0	0	0	0	0	0	25	75	0	0	0
2315	100	0	0	0	0	0	0	25	75	0	0	0
2316	100	0	0	0	0	0	0	25	75	0	0	0
2321	0	100	0	0	0	0	0	25	75	0	0	0
2329	100	0	0	0	0	0	0	25	75	0	0	0
2201	100	0	0	0	0	0	0	15	85	0	0	0
2203	0	100	0	0	0	0	0	15	85	0	0	0
2204	0	100	0	0	0	0	0	15	85	0	0	0
2207	18	82	0	0	0	0	0	15	85	0	0	0
2208	28	72	0	0	0	0	0	15	85	0	0	0
2209	80	20	0	0	0	0	0	15	85	0	0	0
2210	50	50	0	0	0	0	0	10	90	0	0	0
2211	17	83	0	0	0	0	0	10	90	0	0	0
2212	100	0	0	0	0	0	0	10	90	0	0	0
2213	0	100	0	0	0	0	0	10	90	0	0	0
2214	0	100	0	0	0	0	0	10	90	0	0	0
2216	0	100	0	0	0	0	0	10	90	0	0	0
2217	0	100	0	0	0	0	0	10	90	0	0	0
2221	0	100	0	0	0	0	0	10	90	0	0	0
2222	0	100	0	0	0	0	0	10	90	0	0	0
2224	16	84	0	0	0	0	0	10	90	0	0	0
2225	69	31	0	0	0	0	0	10	90	0	0	0
2226	10	90	0	0	0	0	0	10	90	0	0	0
2227	8	92	0	0	0	0	0	10	90	0	0	0
2228	29	53	0	5	13	0	0	10	90	0	0	0
2229	34	34	0	11	21	0	0	10	90	0	0	0
2230	23	58	0	7	12	0	0	10	90	0	0	0
2231	1	52	0	18	28	0	0	10	90	0	0	0
2232	0	81	0	10	10	0	0	10	90	0	0	0
2233	30	61	0	4	4	0	0	10	90	0	0	0
2234	13	87	0	0	0	0	0	10	90	0	0	0
2235	0	100	0	0	0	0	0	10	90	0	0	0
2101	0	98	0	0	2	0	0	0	90	10	0	0
2102	1	91	0	1	7	0	0	0	90	10	0	0
2103	0	54	36	0	10	0	0	0	90	10	0	0
2104	0	23	58	0	19	0	0	0	90	10	0	0
2105	5	36	45	0	13	0	0	0	90	10	0	0
2106	16	36	32	0	16	0	0	0	90	10	0	0
2107	14	40	33	0	14	0	0	0	90	10	0	0
2108	2	92	4	0	2	0	0	0	90	10	0	0
2109	0	100	0	0	0	0	0	0	90	10	0	0

LatLon	MODERN						PLIOCENE					
	DES	TUN	EVE	DEC	GRA	RAI	DES	TUN	EVE	DEC	GRA	RAI
2110	0	100	0	0	0	0	0	0	90	10	0	0
2111	0	100	0	0	0	0	0	0	90	10	0	0
2112	3	97	0	0	0	0	0	0	90	10	0	0
2113	39	61	0	0	0	0	0	0	90	10	0	0
2114	0	100	0	0	0	0	0	0	90	10	0	0
2116	0	100	0	0	0	0	0	0	90	10	0	0
2117	1	88	0	1	10	0	0	0	90	10	0	0
2118	0	100	0	0	0	0	0	0	90	10	0	0
2120	0	41	55	2	2	0	0	0	80	20	0	0
2121	2	21	64	2	12	0	0	0	80	20	0	0
2122	1	3	85	2	9	0	0	0	80	20	0	0
2123	2	15	75	5	3	0	0	0	80	20	0	0
2124	17	7	68	2	6	0	0	0	80	20	0	0
2125	17	21	36	7	19	0	0	0	80	20	0	0
2126	4	42	6	33	15	0	0	0	80	20	0	0
2127	3	40	6	30	20	0	0	0	80	20	0	0
2128	3	21	5	54	18	0	0	0	80	20	0	0
2129	2	23	0	42	32	0	0	0	80	20	0	0
2130	3	4	0	55	38	0	0	0	80	20	0	0
2131	3	0	0	56	42	0	0	0	80	20	0	0
2132	3	28	0	42	27	0	0	0	80	20	0	0
2133	0	46	0	27	26	0	0	0	80	20	0	0
2134	0	20	0	38	41	0	0	0	80	20	0	0
2135	0	37	0	28	34	0	0	0	80	20	0	0
2136	2	64	2	6	26	0	0	0	80	20	0	0
2001	7	33	7	0	53	0	0	0	80	20	0	0
2002	0	100	0	0	0	0	0	0	80	20	0	0
2003	0	53	32	0	15	0	0	0	80	20	0	0
2004	0	2	52	0	45	0	0	0	80	20	0	0
2005	14	3	42	0	42	0	0	0	80	20	0	0
2006	14	21	49	0	16	0	0	0	80	20	0	0
2007	4	9	55	28	4	0	0	0	80	20	0	0
2008	6	31	40	17	6	0	0	0	80	20	0	0
2009	5	42	48	0	5	0	0	0	80	20	0	0
2010	0	82	18	0	0	0	0	0	80	20	0	0
2011	4	86	7	0	4	0	0	0	80	20	0	0
2012	6	74	13	0	6	0	0	0	80	20	0	0
2013	2	91	4	0	2	0	0	0	80	20	0	0
2014	0	100	0	0	0	0	0	0	80	20	0	0
2015	0	100	0	0	0	0	0	0	80	20	0	0
2018	0	0	0	100	0	0	0	0	60	25	15	0
2019	0	0	59	41	0	0	0	0	60	25	15	0
2020	0	16	46	37	1	0	0	0	60	25	15	0
2021	0	3	41	56	0	0	0	0	80	20	0	0
2022	0	0	51	49	0	0	0	0	80	20	0	0
2023	0	0	68	32	0	0	0	0	80	20	0	0
2024	12	0	57	28	2	0	0	0	80	20	0	0
2025	22	0	52	14	12	0	0	0	80	20	0	0
2026	12	22	29	18	19	0	0	0	80	20	0	0
2027	17	14	39	12	18	0	0	0	80	20	0	0
2028	22	1	51	16	9	0	0	0	80	20	0	0
2029	23	0	45	29	3	0	0	0	80	20	0	0
2030	13	7	10	70	0	0	0	0	85	15	0	0

LatLon	MODERN						PLIOCENE					
	DES	TUN	EVE	DEC	GRA	RAI	DES	TUN	EVE	DEC	GRA	RAI
2031	14	8	0	78	0	0	0	0	85	15	0	0
2032	14	7	0	79	0	0	0	0	85	15	0	0
2033	8	17	1	58	16	0	0	0	85	15	0	0
2034	3	28	3	27	40	0	0	0	85	15	0	0
2035	7	30	5	5	52	0	0	0	85	15	0	0
2036	4	64	4	0	29	0	0	0	85	15	0	0
1906	6	5	83	0	6	0	0	0	80	20	0	0
1907	5	4	70	3	18	0	0	0	80	20	0	0
1908	4	1	15	15	65	0	0	0	80	20	0	0
1909	4	3	39	9	45	0	0	0	80	20	0	0
1910	0	14	85	0	0	0	0	0	80	20	0	0
1911	2	25	64	5	2	0	0	0	80	20	0	0
1912	8	2	75	7	8	0	0	0	80	20	0	0
1913	12	10	64	2	12	0	0	0	80	20	0	0
1914	6	0	88	0	6	0	0	0	80	20	0	0
1918	0	0	0	100	0	0	0	0	30	60	10	0
1919	0	0	0	100	0	0	0	0	30	60	10	0
1920	0	0	15	85	0	0	0	0	30	60	10	0
1921	0	0	31	65	4	0	0	0	45	55	0	0
1922	0	3	12	55	29	0	0	0	50	50	0	0
1923	0	0	0	18	82	0	0	0	50	50	0	0
1924	20	0	0	17	63	0	0	0	65	15	20	0
1925	15	0	4	4	77	0	0	0	65	15	20	0
1926	4	0	0	1	95	0	0	0	65	15	20	0
1927	2	0	6	0	92	0	0	0	65	15	20	0
1928	22	4	18	20	37	0	0	0	65	15	20	0
1929	7	2	16	34	40	0	0	0	65	15	20	0
1930	9	1	14	35	41	0	0	0	85	10	5	0
1931	4	0	0	40	55	0	0	0	85	10	5	0
1932	7	2	10	74	6	0	0	0	90	10	0	0
1933	13	2	36	47	2	0	0	0	90	10	0	0
1935	15	6	22	3	54	0	0	0	90	10	0	0
1807	9	0	42	2	44	3	0	0	70	15	15	0
1808	12	0	23	2	63	1	0	0	65	5	30	0
1809	1	0	1	2	95	0	1	0	1	2	95	0
1810	0	0	7	50	43	0	0	0	7	50	43	0
1811	0	0	1	99	0	0	0	0	1	99	0	0
1812	0	0	7	93	0	0	0	0	7	93	0	0
1813	0	0	66	34	0	0	0	0	66	34	0	0
1818	20	0	34	46	0	0	0	0	50	40	10	0
1819	15	0	35	46	4	0	0	0	50	40	10	0
1820	6	0	17	69	7	0	0	0	30	60	10	0
1821	5	0	7	78	10	0	0	0	30	60	10	0
1822	7	0	12	30	50	0	5	0	30	25	40	0
1823	2	0	2	35	62	0	5	0	30	15	50	0
1824	44	0	5	21	29	0	25	0	45	20	20	0
1825	74	0	0	11	14	0	35	0	45	10	10	0
1826	75	0	0	9	16	0	35	0	45	10	10	0
1827	46	0	0	4	50	0	25	0	45	10	25	0
1828	76	0	0	3	22	0	35	0	45	10	10	0
1829	50	0	0	4	46	0	20	0	45	5	30	0
1830	18	0	0	5	77	0	10	0	60	5	25	0
1831	1	0	11	28	60	0	0	0	60	20	20	0

LatLon	MODERN						PLIOCENE					
	DES	TUN	EVE	DEC	GRA	RAI	DES	TUN	EVE	DEC	GRA	RAI
1832	0	0	37	51	12	0	0	0	60	35	5	0
1833	0	0	51	49	0	0	0	0	50	50	0	0
1707	22	0	13	7	45	12	10	0	55	5	30	0
1708	26	0	18	5	52	0	10	0	55	5	30	0
1709	1	0	0	6	93	0	1	0	0	6	93	0
1710	0	0	0	96	4	0	0	0	0	96	4	0
1711	1	0	2	97	1	0	1	0	2	97	1	0
1718	27	0	48	0	24	0	10	0	30	20	40	0
1719	42	0	17	0	40	0	20	0	20	10	50	0
1720	61	0	8	1	30	0	30	0	25	5	40	0
1721	24	0	23	9	44	0	10	0	30	5	55	0
1722	30	0	27	4	38	0	15	0	35	5	45	0
1723	26	0	12	1	62	0	10	0	15	5	70	0
1724	11	0	7	6	76	0	5	0	10	5	80	0
1725	32	0	2	3	64	0	15	0	10	5	70	0
1726	23	0	5	4	69	0	10	0	10	5	75	0
1727	73	0	4	0	22	1	35	0	15	5	45	0
1728	77	0	0	1	23	0	35	0	15	5	45	0
1729	21	0	7	3	70	0	10	0	15	5	70	0
1730	5	0	8	58	27	2	0	0	15	60	25	0
1731	0	0	0	95	5	0	0	0	10	90	0	0
1732	0	0	31	58	10	0	0	0	20	80	0	0
1733	0	0	38	51	11	0	0	0	40	60	0	0
1607	15	0	8	12	65	0	15	0	25	10	50	0
1608	61	0	10	13	16	0	15	0	25	10	50	0
1609	44	0	1	15	40	0	15	0	25	10	50	0
1610	0	0	0	81	19	0	0	0	0	81	19	0
1611	0	0	0	80	20	0	0	0	0	80	20	0
1618	71	0	0	0	29	0	35	0	10	5	50	0
1619	100	0	0	0	0	0	50	0	5	5	40	0
1620	94	0	1	0	5	0	50	0	5	5	40	0
1621	88	0	1	0	11	0	45	0	0	5	50	0
1622	82	0	2	0	15	0	40	0	5	5	50	0
1623	91	0	0	0	8	0	45	0	0	5	50	0
1624	66	0	3	0	31	0	30	0	5	5	60	0
1625	41	0	3	1	55	0	20	0	5	5	70	0
1626	56	0	0	9	33	0	25	0	0	15	60	0
1627	11	0	5	47	34	3	5	0	5	45	40	5
1628	13	0	4	12	34	36	5	0	10	20	30	35
1629	5	0	44	5	19	27	0	0	35	10	25	30
1630	1	0	44	8	15	32	0	0	35	10	25	30
1631	0	0	51	18	17	14	0	0	40	20	25	15
1503	35	0	65	0	0	0	0	0	65	0	35	0
1508	52	0	7	9	3	29	25	0	10	15	5	45
1509	43	0	11	9	19	18	20	0	15	15	15	35
1510	12	0	3	11	8	67	5	0	5	15	5	70
1511	8	0	0	8	81	3	5	0	10	25	50	10
1512	0	0	0	19	6	75	0	0	0	20	5	75
1517	76	0	0	15	8	0	35	0	10	35	20	0
1518	90	0	0	3	7	0	45	0	5	30	20	0
1519	82	0	0	0	18	0	40	0	5	20	35	0
1520	86	0	0	0	14	0	40	0	5	20	35	0
1521	83	0	0	1	15	0	40	0	5	20	35	0

LatLon	MODERN						PLIOCENE					
	DES	TUN	EVE	DEC	GRA	RAI	DES	TUN	EVE	DEC	GRA	RAI
1522	99	0	0	1	0	0	50	0	5	15	30	0
1523	85	0	3	4	6	3	45	0	5	15	30	5
1524	97	0	0	3	0	0	50	0	5	15	30	0
1525	94	0	0	6	0	0	50	0	5	15	30	0
1526	27	0	0	47	21	6	15	0	0	55	25	5
1527	7	0	0	52	40	0	5	0	0	55	40	0
1528	0	0	0	30	18	52	0	0	0	30	15	55
1529	4	0	1	17	10	68	0	0	5	15	10	70
1530	1	0	2	3	33	61	0	0	15	10	10	65
1531	0	0	12	9	3	76	0	0	15	5	0	80
1410	0	0	20	7	12	60	0	0	20	15	5	60
1411	12	0	0	2	0	86	0	0	0	10	0	90
1412	11	0	0	24	22	43	5	0	0	30	20	45
1413	0	0	0	21	35	44	0	0	0	20	30	50
1417	14	0	0	26	60	0	5	0	0	40	50	0
1418	18	0	1	26	49	6	10	0	5	35	40	10
1419	7	0	2	8	80	2	0	0	5	25	60	10
1420	2	0	0	0	98	2	0	0	0	25	70	5
1421	9	0	0	3	89	0	5	0	0	25	70	0
1422	18	0	0	4	79	0	10	0	10	20	60	0
1423	43	0	6	13	33	5	20	0	20	25	30	5
1424	37	0	0	16	47	0	20	0	20	25	30	5
1426	0	0	0	0	0	100	0	0	0	0	0	100
1427	8	0	0	13	57	23	5	0	0	15	50	25
1429	7	0	0	12	27	54	5	0	0	15	25	55
1430	13	0	2	23	49	12	5	0	5	25	45	20
1431	0	0	0	0	0	100	0	0	0	0	0	100
1432	0	0	0	0	0	100	0	0	0	0	0	100
1311	0	0	0	0	0	100	0	0	0	0	0	100
1312	0	0	0	14	30	56	0	0	0	14	30	56
1313	0	0	0	4	20	76	0	0	0	4	20	76
1314	0	0	0	0	26	74	0	0	0	0	26	74
1318	3	0	6	0	24	66	3	0	6	0	25	66
1319	0	0	0	0	31	69	0	0	0	0	31	69
1320	0	0	0	0	27	73	0	0	0	0	27	73
1321	0	0	0	0	37	63	0	0	0	0	37	63
1322	1	0	0	1	74	23	1	0	0	1	74	23
1323	31	0	0	24	43	1	15	0	0	40	40	5
1324	27	0	0	27	46	0	15	0	0	40	40	5
1327	0	0	0	0	0	100	0	0	0	0	0	100
1329	0	0	0	0	0	100	0	0	0	0	0	100
1330	0	0	0	0	0	100	0	0	0	0	0	100
1331	0	0	0	0	0	100	0	0	0	0	0	100
1332	0	0	0	0	0	100	0	0	0	0	0	100